RECEIVED BY OSTI MAY 06 1985

CONF-8503120--7

LA-UR--85-1511

DE85 010724

TITLE: EXPERIMENTS ON η-MESON PRODUCTION

AUTHOR(S) J. C. Peng

SUBMITTED TO. AIP Conference Proceedings, Conference held at Tempe, AZ, March 10-14, 1985

EXPERIMENTS ON η-MESON PRODUCTION

J. C. Peng
Los Alamos National Laboratory, Los Alamos, NM 87545

ABSTRACT

Following a review of some highlights of η-meson characteristics, the status of η-meson production experiments is reviewed. The physics motivations and first results of two LAMPF experiments on (π,η) reactions are discussed. Possible future experiments are also discussed.

1. INTRODUCTION

The existence of several meson factories has greatly advanced our knowledge of pion-nucleus interactions. At the same time, the relatively low intensity kaon beams from several proton-synchrotron accelerators have also provided a first glance at the kaon-nucleus and hyperon-nucleus interactions. In contrast, the roles of heavy mesons (η, ω, ρ, σ, etc.) in nuclear physics have received little attention up to now. Very little information exists on the interaction between these heavy mesons with nucleons, and almost nothing is known about their interactions with nuclei. Some of the motivations for studying these heavy mesons, in the context of medium energy nuclear physics, are the following: First, the microscopic structures of these mesons are distinct from those of the more familiar pions and kaons. A comparative study of the response of these various mesons in the nuclear environment could reveal phenomena which can only be understood by the subatomic (quark and gluon) degrees of freedom. Second, the heavy mesons are responsible for nuclear forces at intermediate and short distances in the conventional One Boson Exchange (OBE) models. The advent of QCD advocates explicit consideration of quarks and gluons at such short distances. A better knowledge of the nature of heavy mesons in a nuclear medium can help to reconcile these two apparently different approaches. Third, various theoretical models devised to describe phenomenologies in the pion-nucleus interaction could be significantly tested by their ability to describe various aspects in the interactions of heavier mesons with nuclei.

In this paper, we will discuss some η-meson production experiments being pursued at LAMPF. The physics motivations of these experiments and other possible future experiments will be presented. Some of the physics issues in η-meson production are common issues in the production of all heavy mesons. In this respect, the η-meson production experiments could serve as a prototype for future studies of heavy meson production.

We will first summarize briefly some pertinent properties of the η-meson. The current status of η-meson production on proton and on nuclear targets will then be reviewed. The physics motivations and some first results of η-meson production experiments at LAMPF will be discussed.

2. HIGHLIGHTS OF η-MESON PROPERTIES

A. Comparison between η and π^0

The η-meson is a pseudoscalar meson classified in the same SU(3) octet as pions and kaons. Figure 1 shows that the η-meson occupies the same location in the SU(3) diagram as the π^0. It is instructive to compare the properties[1] of the η-meson with those of the more familiar π^0-meson, as shown in Table I. Both mesons have the same quantum numbers of spin, parity, and charge parity ($J^{PC} = 0^{-+}$). The major difference is in the isospin ($I = 1$ for π^0, $I = 0$ for η). This difference is reflected in their quark wave functions; while both π^0 and η have the $u\bar{u}$ and $d\bar{d}$ (they couple to $I = 0,1$) components, only η contains the $s\bar{s}$ (it couples to $I = 0$ only) component. The conventional wisdom about strange quarks being more massive than the up and down quarks is consistent with the fact that η is four times heavier than π^0. With the absence of strong decays, the lifetime of η is relatively long. Analogous to π^0, η decays through electromagnetic interactions with the 2γ emission being the most dominant channel. However, the larger available phase space leads to a shorter lifetime for η, as well as a larger variety of decay channels.

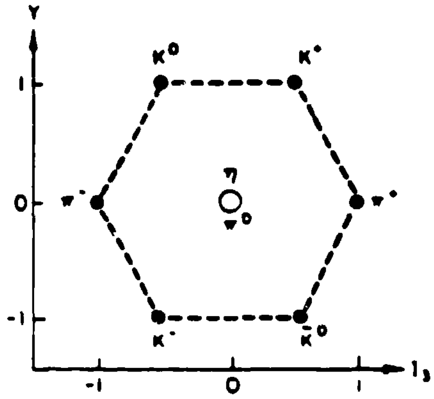

Fig. 1. SU(3) pseudoscalar meson octet diagram.

Table I. Comparison between η and π^0 mesons

	η	π^0
J^{PC}	0^{-+}	0^{-+}
(I, I_z)	(0,0)	(1,0)
Quark w.f.	$(u\bar{u}+d\bar{d}-2s\bar{s})/\sqrt{6}$	$(u\bar{u}-d\bar{d})/\sqrt{2}$
Mass	548.8 MeV	134.9 MeV
Mean life	0.75×10^{-18} sec	0.83×10^{-16} sec
B.R. of 2γ decay	39%	98.8%

B. Quark Contents of η

The quark wave function of η listed in Table I is for a pure SU(3) meson octet. As SU(3) is only an approximate symmetry, the physically observed η-meson is a mixture of η_8 and η_1, which are the SU(3) octet and singlet states:

$$\eta = \eta_8 \cos \theta_p - \eta_1 \sin \theta_p$$

$$\eta' = \eta_8 \sin \theta_p + \eta_1 \cos \theta_p \qquad (1)$$

$$\eta_8 = \frac{1}{\sqrt{6}} (u\bar{u} + d\bar{d} - 2s\bar{s}) \; , \; \eta_1 = \frac{1}{\sqrt{3}} (u\bar{u} + d\bar{d} + s\bar{s})$$

The pseudoscalar meson mixing angle θ_p is determined to be about -10° from the Gell-Mann-Okubo[2] mass formula, and also from the comparison[3] of $\Gamma(\pi^0 \to 2\gamma)$ with $\Gamma(\eta \to 2\gamma)$.

A further complication arises from isospin-violating interactions causing mixing between η and π^0. Dalitz and Von Hippel estimate[4] the mixing angle $\lambda_{\eta\pi^0}$ to be 0.61° from the following relation:

$$\lambda_{\eta\pi^0} = 3^{-1/2}(m^2_{\pi^0} - m^2_{\pi^+} + m^2_{K^+} - m^2_{K^0})/(m^2_{\pi^0} - m^2_{\eta})$$

Gross et al.[5] also relate this mixing angle to the mass difference of the up and down quarks:

$$\sin \lambda_{\eta\pi^0} = 3^{1/2}(m_d - m_u)/4m_s$$

The observation of the $\psi(3685) \to \pi^0\psi$ decay was considered[6] evidence of η-π^0 mixing. Cutkosky suggested[7] that a careful measurement of the $\pi^- p$ charge exchange reaction around the η threshold could identify effects due to this mixing. It remains an interesting and challenging task to investigate the η-π^0 mixing.

In principle, the η-meson can also contain charm quarks through the mixing between η and η_c. Indeed, this mixing was invoked[8] to explain the anomalously large branching of the $\psi'(3685) \to \psi\eta$ decay (B.R. = 2.8 ± 0.6%).

Although the exact quark contents of η are still somewhat uncertain, it can be concluded that η contains $u\bar{u}$, $d\bar{d}$, $s\bar{s}$, and possibly $c\bar{c}$, with $s\bar{s}$ being the most dominant component.

Table II. η decay modes

Decay Channel	Fraction
$\gamma\gamma$	$(39.0 \pm 0.8)\%$
$3\pi^0$	$(31.8 \pm 0.8)\%$
$\pi^0\gamma\gamma$	$(0.10 \pm 0.02)\%$
$\pi^+\pi^-\pi^0$	$(23.7 \pm 0.5)\%$
$\pi^+\pi^-\gamma$	$(4.91 \pm 0.13)\%$
$e^+e^-\gamma$	$(0.50 \pm 0.12)\%$
$\mu^+\mu^-\gamma$	$(3.1 \pm 0.4) \times 10^{-4}$
e^+e^-	$(<3) \times 10^{-4}$
$\mu^+\mu^-$	$(6.5 \pm 2.1) \times 10^{-6}$
$\pi^+\pi^-e^+e^-$	$(0.13 \pm 0.13)\%$
$\pi^+\pi^-\gamma\gamma$	$(<0.21)\%$
$\pi^+\pi^-\pi^0\gamma$	$(<6) \times 10^{-4}$
$\pi^+\pi^-$	$(<0.15)\%$
$\pi^0e^+e^-$	$(<5) \times 10^{-5}$
$\pi^0\mu^+\mu^-$	$(<5) \times 10^{-6}$
$\pi^0\mu^+\mu^-\gamma$	$(<3) \times 10^{-6}$

C. Decay Modes of η

Table II shows the most recent tabulation[1] of the branching ratios of various decay modes of the η-meson. Although the η-meson is sufficiently massive to decay into three pions, the $\eta \to 3\pi$ decay violates G-parity and proceeds via electromagnetic interaction. The $\eta \to 2\pi$ decay is both P and CP violated. The $\eta \to 2\gamma$ and $\eta \to 3\pi$ decays are the two most dominant electromagnetic decay channels. As η is a self-conjugate particle, the decay of η provides an interesting test ground for searching for possible charge-conjugation (C) violation in electromagnetic interactions. In particular, any difference between the π^+ and π^- energy spectra in the $\eta \to \pi^+\pi^-\pi^0$ and $\eta \to \pi^+\pi^-\gamma$ decays would be good evidence of C-violation. In fact, early experiments[9] did show some evidence of C-violation; however, these early results were not supported by later experiments.[10] More accurate experiments would be worthwhile for settling this important issue.

It appears that there is room for improvement on several η-decay modes. For example, the $\eta \to \pi^0\gamma\gamma$ decay was thought to have a branching of 3% until a recent experiment[11] showed that the branching is only 0.1%. The upper limit of the $\eta \to \pi^+\pi^-$ is only determined[12] at 0.15%, and the $\eta \to e^+e^-$ decay[13] has not been observed yet.

D. <u>ηN Scattering Length and Coupling Constant</u>

Our current knowledge about the η-nucleon interaction is very limited. One can make a simple observation that, unlike the πN system which couples to both the Δ^* and N^* resonances, the ηN system only couples to the I = 1/2, N^* resonances. Several N^* resonances actually have ηN as an important decay channel, as shown[1] in Table III.

Table III. Coupling between N^* and ηN

Resonance	J^P	L_{2I2J}	ηN Branching
$N^*(1440)$	$1/2^+$	P_{11}	8-18%
$N^*(1535)$	$1/2^-$	S_{11}	~35%
$N^*(1710)$	$1/2^+$	P_{11}	~25%

The $\pi^-p \to \eta n$ and the $K^-p \to \eta\Lambda$ reactions have been analyzed[14] to deduce the ηN and $\eta\Lambda$ interactions. In particular, the scattering length has been calculated and the possibility of ηN bound or resonant states was discussed. In a K-matrix analysis, Tuan[14] calculated the ηN scattering length to be $a = 0.83 + i0.05$ fm. Bhalerao and Liu,[15] using an isobar model to analyze all available $\pi^-p \to \eta n$ data, obtained very recently an ηN scattering length of $a = 0.28 + i0.19$ fm. In both analyses, an <u>attractive</u> interaction between η and nucleon is deduced. This situation is distinct from that of the low energy πN and KN interaction,[16] where scattering lengths imply a repulsive interaction.

One quantity relevant to the strength of the ηN interaction is the coupling constant $G_{\eta NN}$. Several methods have been used to determine the magnitude of $G_{\eta NN}$. In the SU(3) model, $G_{\eta NN}$ is related to the well determined πN coupling constant $G_{\pi NN}$ through the relation[16]

$$G_{\eta NN} = 3^{-1/2} G_{\pi NN}(3-4\alpha) \quad ; \quad \alpha = D/(D + F) \qquad (2)$$

where α is the fraction of D-type SU(3) octet coupling. From hyperon decay experiments,[17] α is determined to be between 0.60 and 0.66. This gives a value of $G^2_{\eta NN}/G^2_{\pi NN}$ between 0.043 and 0.12. Another method used to determine $G_{\eta NN}$ is from the ratio of the back-angle cross sections of the reactions $\pi^-p \to \eta n$ and $\pi^-p \to \pi^0 n$[18] (or $K^-p \to \eta\Lambda$ and $K^-p \to \pi^0\Lambda$).[19] If one assumes that the backward-produced η and π^0 in these reactions are dominated by nucleon exchange, then $G^2_{\eta NN}/G^2_{\pi NN} = \sigma(\pi^-,\eta)/\sigma(\pi^-,\pi^0)$. This method gives a value of 0.18 to

0.45 for $G^2_{\eta NN}/G^2_{\pi NN}$. Finally, from the fit to low energy nucleon-nucleon scattering data in the One Boson Exchange model, the ηN coupling constant is given as $G^2_{\eta NN}/G^2_{\pi NN} = 0.29$ in the most recent tabulation.[16] It can be summarized that $G_{\eta NN}$ is not yet well determined. However, all evidence so far points to a significantly weaker ηN coupling than the πN coupling.

It is also of interest to examine the role of η-meson in nuclear force. In the One Boson Exchange model, the η-meson can contribute to the spin-spin interaction and tensor force

$$V_\eta(r) = \sigma_1 \cdot \sigma_2 \, V^\eta_\sigma(r) + S_{12} \, V^\eta_T(r) \tag{3}$$

As a result of the large mass of η and the small ηN coupling, the contribution of η-meson exchange in the NN force is small and not clearly identified.[20] A similar situation has also been found in the hyperon-nucleon interaction[21] and the $\bar{N}$N interaction.[22] It appears that the η-meson plays a rather insignificant role in the OBE model to account for nuclear forces.

3. η-MESON PRODUCTION ON PROTON AND NUCLEAR TARGETS

A. The $\pi^-p \rightarrow \eta n$ Reaction

Table IV lists the threshold energies for various projectiles to produce η-mesons on proton. The proton-induced η-production involves three-body final states making it not so desirable experimentally. The kaon-induced reaction suffers from the low beam intensity and a small cross section. A more favorable reaction for η-meson production is the $\pi^-p \rightarrow \eta n$ reaction. As shown in Fig. 2, the integrated cross section[23] of this reaction rises rapidly once the pion momentum is above the threshold, reaching a maximal cross section of 3 mb around 800 MeV/c before falling gradually as the pion momentum further increases.

Table IV. Elementary processes for η-production

Reaction	Threshold
$p + p \rightarrow \eta + p + p$	1982 MeV/c
$\pi^- + p \rightarrow \eta + n$	686 MeV/c
$K^- + p \rightarrow \eta + \Lambda$	719 MeV/c
$\gamma + p \rightarrow \eta + p$	710 MeV/c

Figure 3 shows that at energies slightly above threshold the angular distributions[24,25] of the (π,η) reaction are nearly isotropic, reflecting the dominance of S-wave production near threshold. The coupling to the N^*(1535) S11 resonance is responsible for this s-wave dominance. A recent analysis[15] using an off-shell isobar model gives an excellent description of the $\pi^-p \rightarrow \eta n$ differential cross sections.

B. η-Meson Production on Nuclear Targets

There exist only a few η-meson production experiments on nuclear targets. About half a dozen experiments[26,27] of the (π,η) reaction on nuclear targets have been reported so far. These experiments all have the common features that very high energy pion beams were used to measure inclusive (π,η) cross sections. No attempts to measure

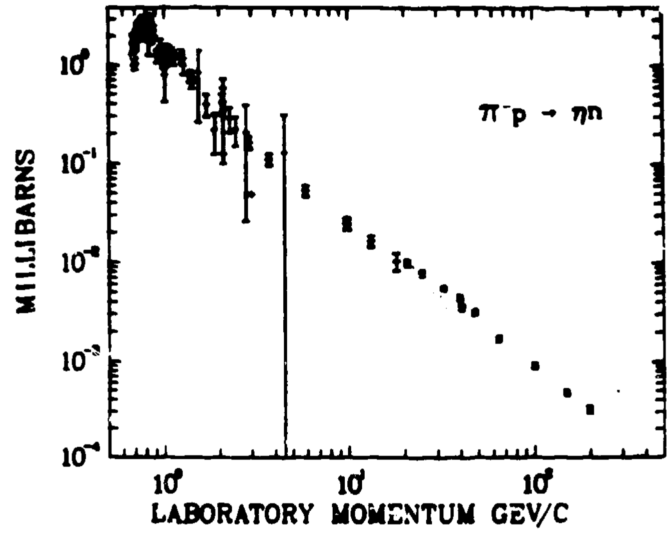

Fig. 2. Integrated cross section of the $\pi^- p \to \eta n$ reaction.[23]

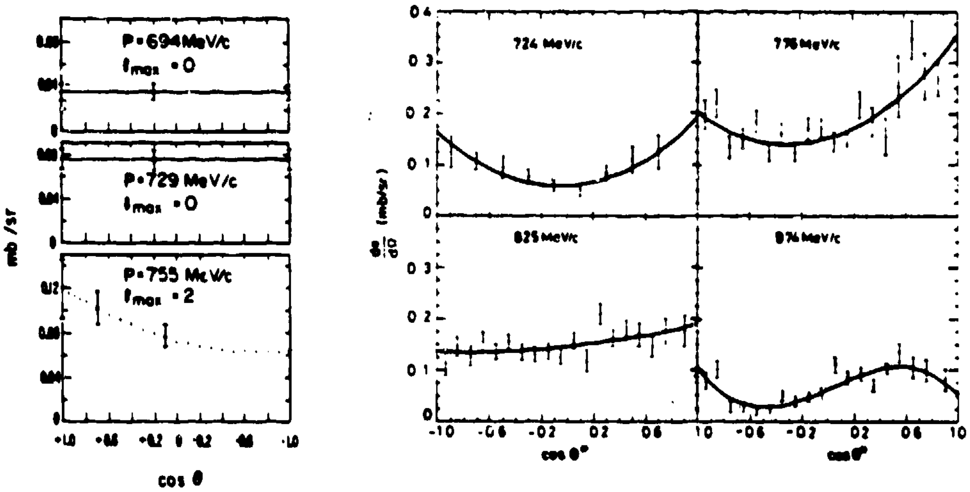

Fig. 3. Angular distributions of the $\pi^- p \to \eta n$ reaction from Refs. 24 and 25.

discrete nuclear states have been made. Figure 4 shows the inclusive cross section $d\sigma/dt(\pi^-, \eta)$ on a number of nuclear targets measured by Guisan et al.[26] The shape of the differential cross section does not vary noticeably with the target mass. However, the magnitude of the cross section increases steadily with the target mass. From this mass dependence, the ηN total cross section $\sigma(\eta N)$ can be deduced. This method has also been used to determine[27] the total cross sections of other short-lived mesons such as ρ, ω, and f. Figure 5 shows a tabulation of $\sigma_t(\eta N)$ determined from the existing η-production experiments on nuclei. the ηN total cross sections are observed to be significantly smaller than the πN cross section (dashed curve), but in rather good agreement with the prediction of additive quark model (solid curve):[28]

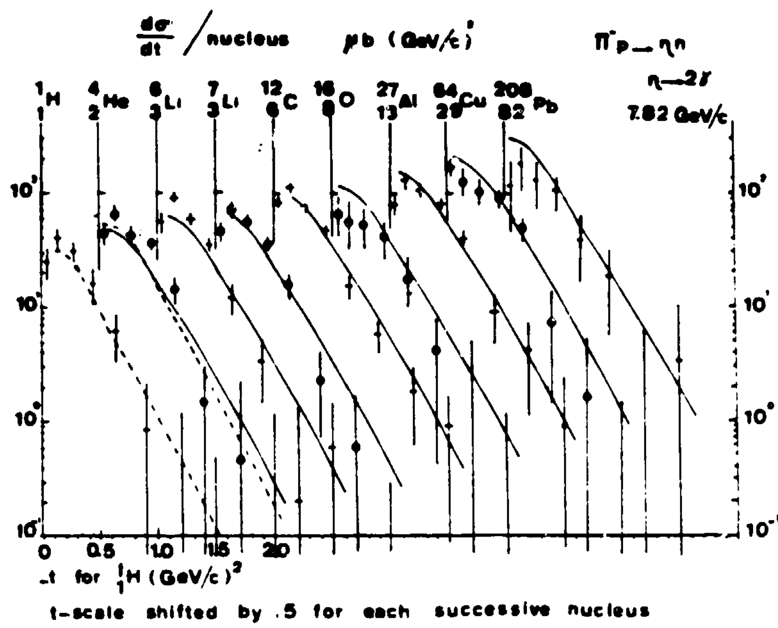

Fig. 4. Inclusive (π,η) cross sections measured on nuclear targets from Ref. 26.

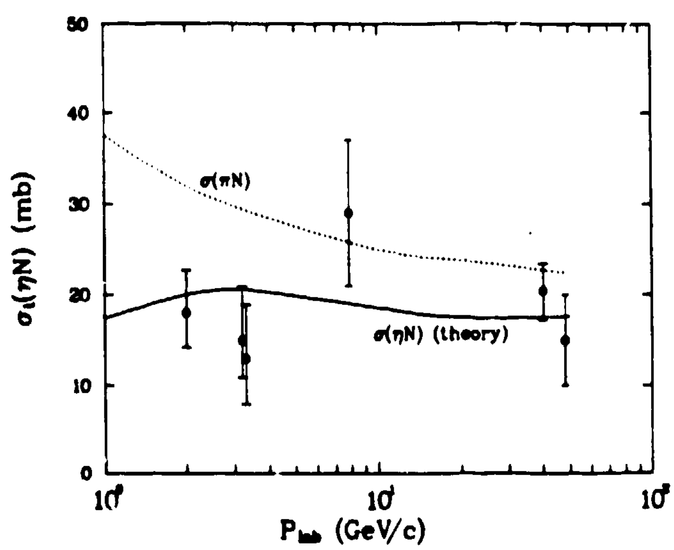

Fig. 5. ηN total cross section determined from inclusive η-production experiments.

$$\sigma_{\eta N} = (\sigma_{K^+p} + \sigma_{K^-p} + \sigma_{K^+n} + \sigma_{K^-n})/3 - (\sigma_{\pi^+p} + \sigma_{\pi^-p})/6 \qquad (4)$$

The back-angle cross section of a proton-induced η-production reaction pd $\rightarrow$ ^{3}Heη has been measured at several beam energies.[29,30] Figure 6 shows that the back-angle cross section increases at lower beam energies. In fact, the three low energy data points were measured below the pp $\rightarrow$ ppη threshold.

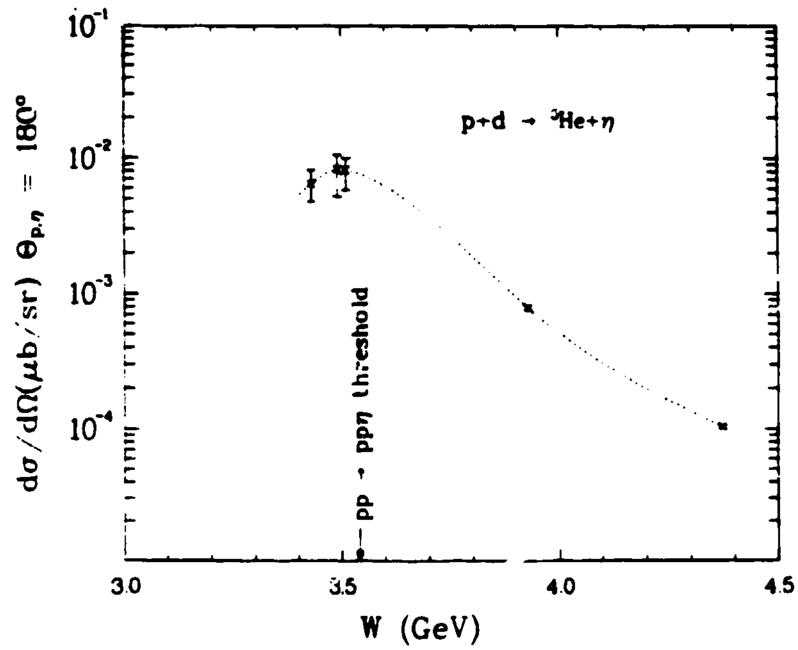

Fig. 6. Back-angle cross sections of the P + d → ^{3}He + η reaction. The curve is drawn through the data.

4. (π,η) EXPERIMENTS AT LAMPF

In this section we will discuss two LAMPF proposals[31,32] on (π,η) reactions. The physics motivations and some first results of these experiments will be presented.

A. Physics Motivations

There are several ways to look at the ($\pi^\pm$,η) reactions on nuclei. First, they can be viewed as a charge exchange reaction similar to the ($\pi^\pm$,π^0) or (p,n) reactions. Indeed, from the similarity between π^0 and η discussed earlier, it is plausible that the ($\pi^\pm$,η) reactions could bear some resemblances to the ($\pi^\pm$,π^0) reactions. However, unlike ($\pi^\pm$,π^0), the ($\pi^\pm$,η) reactions involve two particles belonging to different isospin multiplets. Therefore, the charge-exchange mechanism in the ($\pi^\pm$,η) reaction could be different from that of ($\pi^\pm$,π^0). Another important distinction between ($\pi^\pm$,η) and the usual charge-exchange reactions is the large mass difference between $\pi^\pm$ and η, which implies a relatively large momentum transfer (~250 MeV/c) even at small reaction angles. In view of the similarities and differences between the ($\pi^\pm$,η) and the ($\pi^\pm$,π^0) reactions, it would be interesting to compare ($\pi^\pm$,η) data with the extensive ($\pi^\pm$,π^0) data already obtained at LAMPF.

The ($\pi^\pm$,η) reactions can also be considered as coherent production of the η-meson, analogous to pion[33] or kaon[34] coherent productions. A study of the coherent η-production mechanism might shed some light on the problem of coherent π-production, especially below the free threshold.[35] The threshold of the ($\pi^\pm$,η) reactions is significantly lowered on nuclear targets. As an example, the threshold of the ^{3}He(π^-,η)t reaction is 583 MeV/c, more than 100 MeV/c lower than the free threshold. An interesting feature of the (π,η) reaction is shown in Fig. 2. The (π,η) cross section rises rapidly toward the maximal value once the pion momentum is above the threshold. This "step function" behavior implies a very sensitive dependence of the subthreshold η-production yield on the momentum distribution of nucleons in nuclei. Therefore, the subthreshold (π,η) reaction could be a sensitive tool to measure the high energy tail of the nucleon momentum distribution.

Another important feature of the $(\pi^{\pm},\eta)$ reactions is that the appearance of η in the exit channel should provide information about the η-nucleus interaction, which is unknown at present. The η-nucleus distortion in the exit channel should affect the shape and magnitude of the differential cross sections, and a quantitative analysis should lead to useful information about this interaction.

While it would be most exciting if $(\pi^{\pm},\eta)$ reactions can populate selectively some discrete states (such as IAS in the (π^+,η) reaction), it would be very interesting nevertheless to study the inclusive η-production as a function of pion momentum and target mass. The rather energetic pions required for the $(\pi^{\pm},\eta)$ reactions have long mean-free-paths and can probe not only the nuclear surface, but also the nuclear interior. From the mass dependence of the inclusive (π,η) cross section, one expects to extract ηN total cross section.

B. Proposed (π,η) Measurements at LAMPF

At the LAMPF P^3 channel, a pion beam up to ~750 MeV/c, about 60 MeV/c above the (π,η) free threshold, can be delivered.[36] This limits the (π,η) reaction to be studied near the free threshold or at subthreshold. Fortunately, the peaking of the (π,η) cross section near the threshold energy and the interest of studying subthreshold (π,η) mechanisms make this limitation unimportant. The π^- flux at The P^3 channel drops rapidly toward high momentum (10^5/sec for 700 MeV/c π^- beam). Fortunately, the more intense π^+ beam can be used for η-production on nuclear targets through the process $\pi^+ n \to \eta p$. In addition, the flux improves rapidly for the lower energy pions used for subthreshold experiments.

In the first (π,η) experiment,[31] we will use the existing LAMPF π^0-spectrometer[37] to measure the two energetic gammas emitted by η-mesons, and the Large Acceptance Spectrometer (LAS)[38] to measure the tritons emitted in the $^3He(\pi^-,\eta)t$ reaction. The $\pi^- p \to \eta n$ reaction, which has been measured at other laboratories,[24,25] will be used to optimize the η-detection system and the characteristics of the P^3 beam line at this relatively high momentum.

We plan to measure angular distributions of the $^3He(\pi^-,\eta)t$ and the $^7Li(\pi^+,\eta)^7Be$ reactions. The $^3He(\pi^-,\eta)t$ reaction has the advantage that the triton ground state can be resolved from the continuum because of a 5 MeV gap between them. Furthermore, a complete angular distribution can be obtained by measuring the recoiling triton with the LAS spectrometers. Figure 7 shows a DWIA prediction by Liu and Bhalerao[39] on the angular distributions of the $^3He(\pi^-,\eta)t$ reaction. Both momenta chosen in the calculations are below the free threshold. The back angle cross sections are predicted to be sensitive to the pion phase shift[40] used in the input.

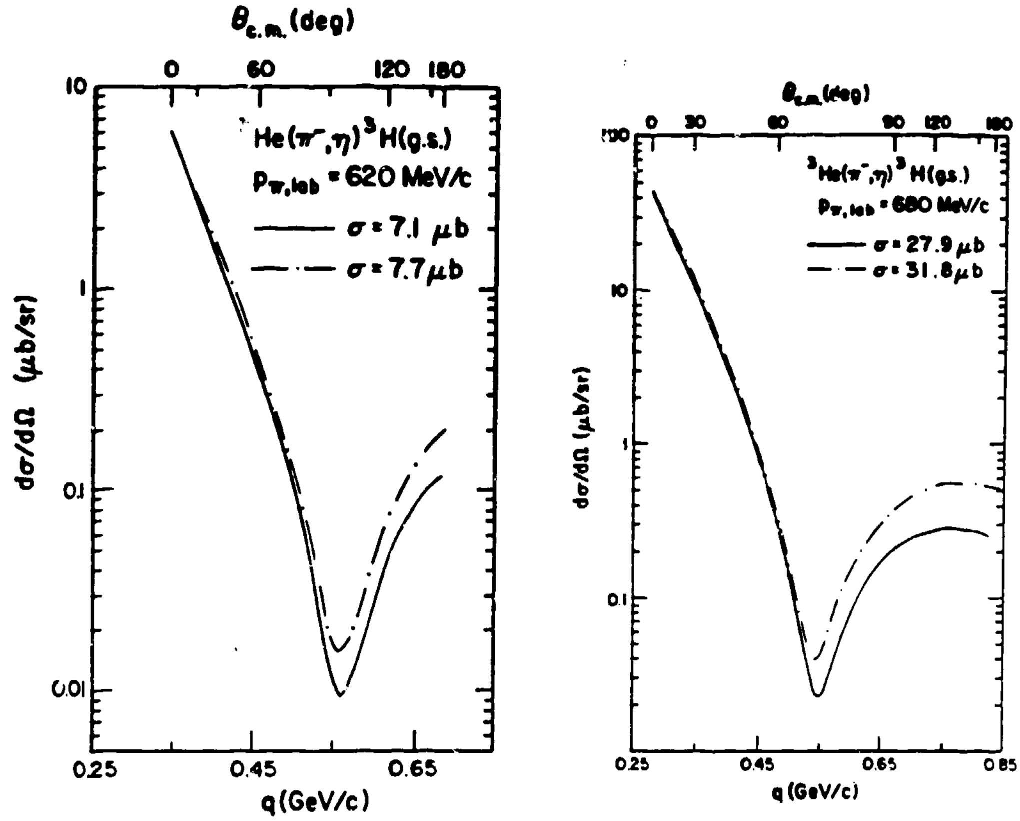

Fig. 7. Predictions of the $^3He(\pi^-,\eta)t$ cross sections from Ref. 39. The two curves correspond to different pion phase shifts.[40]

We also propose to set the π^0-spectrometer at 0° to survey the (π^+,η) reaction on a number of targets ranging from ^7Li to ^{120}Sn. The selectivity, the mass dependence, and the energy dependence of the (π^+,η) reaction should be revealed in these measurements.

In the second (π,η) experiment, we plan to construct an η-spectrometer and concentrate on measuring the inclusive (π,η) cross section on target ranging from deuterium to Ge. The η-spectrometer is identical to the existing LAMPF π^0 spectrometer in terms of the principles of operation. However, we propose to use NaI crystals for the converters and the total absorption counters. This allows us to have a compact spectrometer with roughly the same overall acceptance in solid angle as the LAMPF π^0 spectrometer. In addition, the NaI total absorption counters act independently as high resolution gamma ray detectors.

C. Results of a First (π,η) Test Run

An initial experiment* to measure the (π,η) reaction was performed at the P^3W channel for three days in September 1984. The

*Participants: J. E. Simmons, N. Stein, J. Kapustinsky, D. H. Fitzgerald, T. K. Li, and J. C. Peng.

purpose of this short run was to measure pion flux at relatively high momentum (~700 MeV/c) at the P^3 channel, and to observe the (π,η) reactions for the first time at LAMPF. The experimental setup is shown schematically in Fig. 8. The S1 scintillator is placed in the

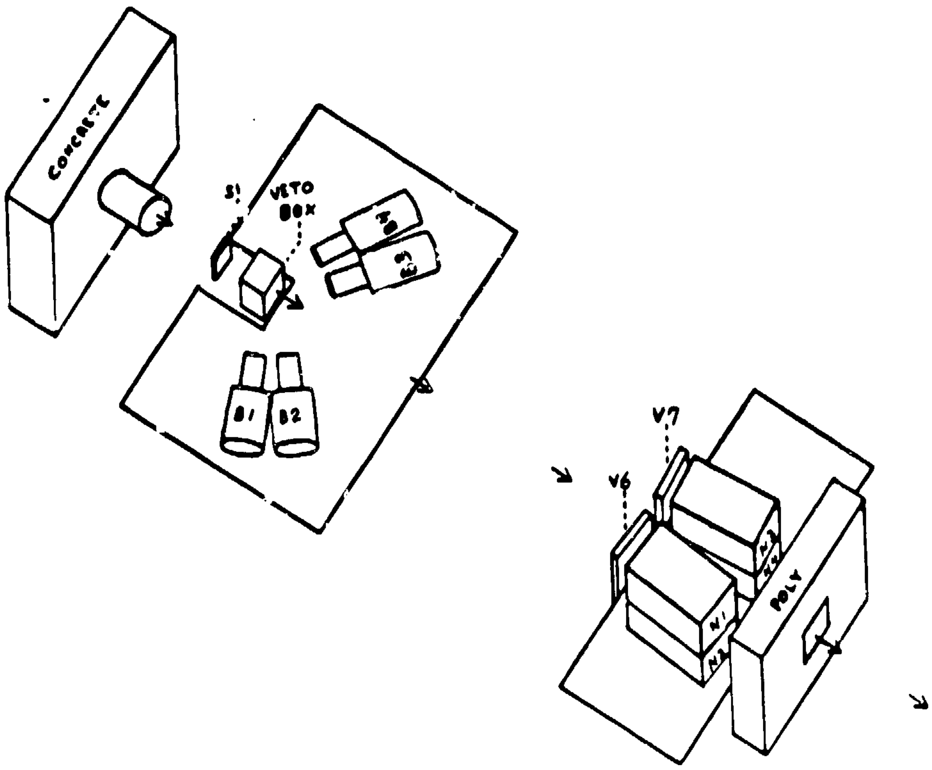

Fig. 8. Experimental setup for the (π,η) test run.

beam to count the incident pions and to provide a start signal for the neutron time-of-flight. Four sets of BGO counters, each a 3-in × 6-in cylinder, are placed at 50° and 70° with respect to the beam direction to measure the coincident gamma rays emitted in the $\eta \to 2\gamma$ decay. Four sets of scintillation counters placed 4 meters from the target detect neutrons from the $\pi^- + p \to n + \eta$ reaction. The target is surrounded by six scintillation counters vetoing events accompanied by charged-particle emission.

From the difference of the CH_2 and carbon target measurements, the $\pi^- + p \to \eta + n$ reaction was measured at 705 MeV/c π^- incident momentum. In addition, inclusive η-meson production was also observed for π^- on ^{12}C target at both 705 MeV/c and 670 MeV/c, the latter momentum being below the free threshold.

With 0.5 mA proton current and a 1% momentum acceptance in the P^3 channel, the π^- flux on S1 is measured to be 0.5×10^5/sec and 3×10^5/sec, respectively, at 705 MeV/c and 670 MeV/c. This is in reasonable agreement with the extrapolation on previous measurements.[41]

Figure 9 shows the neutron TOF spectrum obtained with 705 MeV/c π^- beam on hydrogen (CH_2-C). Four peaks are clearly visible in the spectrum. The peak at the shortest flight time is due to gamma

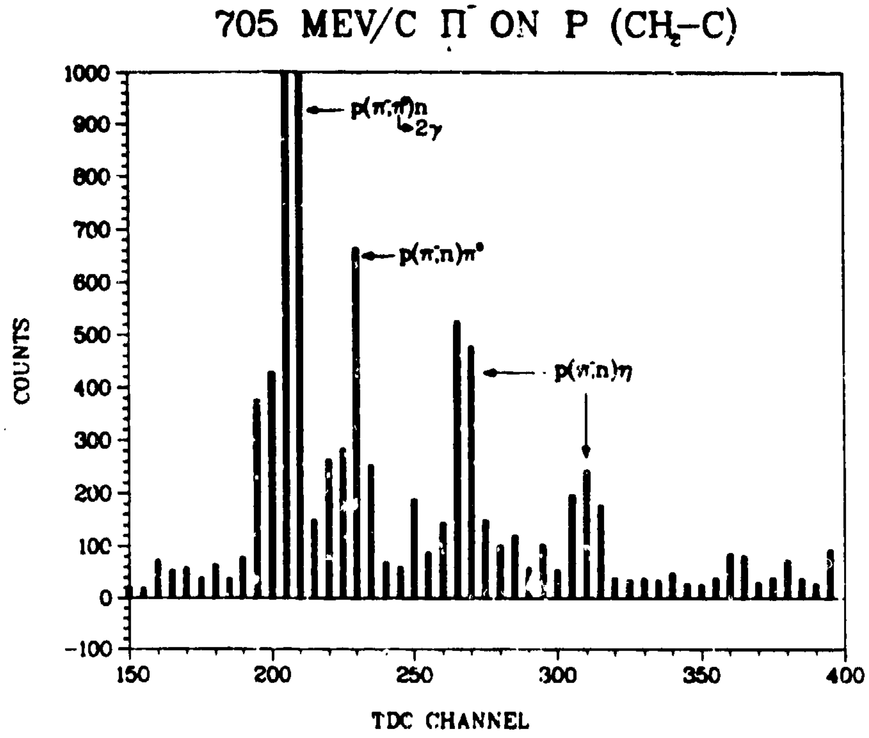

Fig. 9. Time-of-flight spectrum of the neutron counters. 705 MeV/c π^- beam on proton.

flashes. They are attributed mainly to π^0 produced in the $p(\pi^-,\pi^0)n$ reaction. The peak next to the gamma flash corresponds to neutrons coming from the $p(\pi^-,n)\pi^0$ reaction. Finally, the two remaining peaks are identified, from the flight time, as neutrons emitted in the $\pi^- + p \to n + \eta$ reaction. These two peaks correspond to neutrons produced, respectively, at forward and backward angle in the center of mass system. Preliminary results obtained for the cross section of the $p(\pi^-,\eta)\eta$ reaction are 88 μb/sr ($\theta_{c.m.}(\eta) = 144^\circ$) and 86 μb/sr ($\theta_{c.m.}(\eta) = 25^\circ$). This is in good agreement with previous measurements[24] at similar π^- beam energy.

Evidence of η-production has also been observed with the BGO counters. The $\eta \to 2\gamma$ decays are characterized by a coincidence of two energetic gamma rays (E_{tot} > 600 MeV) hitting the left arm (B1,B2) and the right arm (B3,B4) of the BGO detecting system. Invariant mass can be constructed for each of the four left-right pairs of BGO counters. Figure 10 shows the invariant mass plots for 705 MeV/c π^- on CH_2 target. The presence of η-meson is clearly observed in these plots, with the exception of the plot for detectors B2,B3 which subtend too small an opening angle. (The minimal opening angle for 100 MeV η is ~115°, while B2,B3 subtend ~100°.) With this relatively simple gamma-ray detector system, a total of ~500 η events have been identified with ~7 hours of π^- beam.

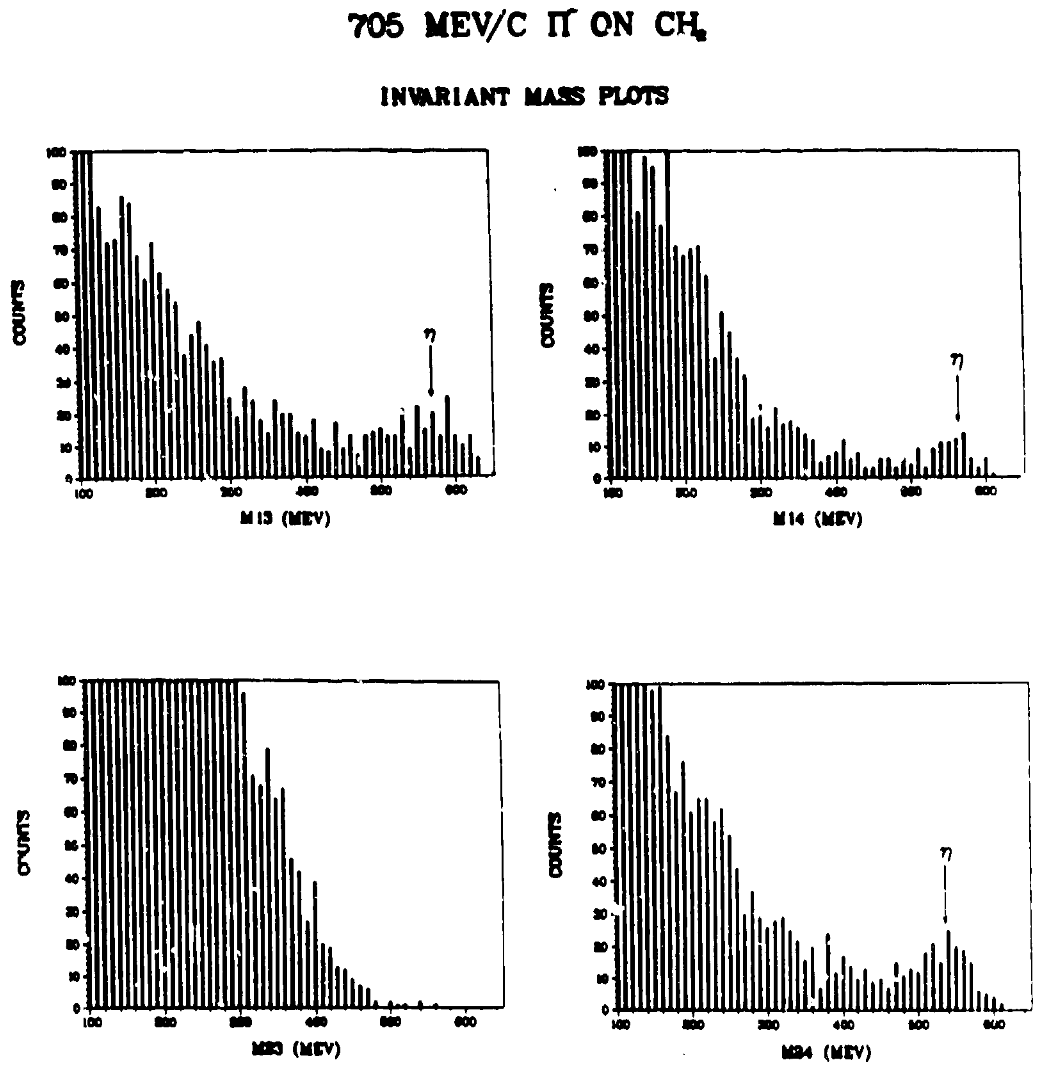

Fig. 10. Invariant mass plots for the four left-right pairs of BGO counters. 705 MeV/c π^- beam on CH_2 target.

The η-production on carbon targets with 705 MeV/c and 670 MeV/c π^- beam has also been observed with the BGO counters. Preliminary results indicate that at 705 MeV/c the η-production rate on ^{12}C target is a factor of 3 lower than on hydrogen target. If this result is confirmed by further analysis and experiments, it could imply a rather strong absorption of η-meson in nucleus at this energy. This is somewhat surprising since the η-nucleon coupling constant was predicted to be much weaker than the π-nucleon coupling constant. Furthermore, inclusive (π,η) reaction measured[26,27] at higher pion momenta show the cross section to increase monotonically with target mass. Another preliminary result obtained in this experiment is that the η-production rate on ^{12}C at 670 MeV/c (subthreshold) is only a factor of two lower than at 705 MeV/c.

5. FUTURE PROSPECTS

From the results of the two LAMPF (π,η) experiments, scheduled to run in the near future, we will be able to judge the full potential of the (π,η) program at LAMPF. We will discuss in the following some possible future experiments[42] on η-meson physics.

As discussed earlier, very poor experimental limits exist on the $\eta \to \pi^+\pi^-$ and $\eta \to e^+e^-$ decay modes. To improve on the accuracy of these decay modes, one needs a more elaborate neutron detector system to tag on the production of η (from the $\pi^-p \to \eta n$ reaction). One important feature of the $\pi^-p \to \eta n$ reaction near threshold energy is that neutrons are emitted in a small forward cone in the lab system. With a 25" × 25" neutron detection system and a 20 cm liquid hydrogen target, an η tagging rate of 2×10^4/hour can be obtained.

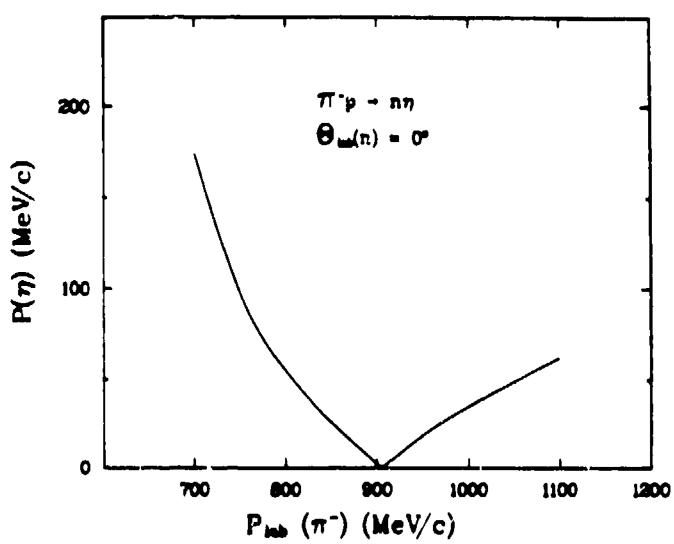

Fig. 11. Momentum of the η meson produced in the $\pi^-p \to \eta n$ reaction, with neutron detected at 0°.

One interesting feature of the $\pi^-p \to \eta n$ reaction (or the $\pi^+n \to \eta p$ reaction) is that η can be produced nearly recoillessly. Figure 11 shows the momentum of η when a neutron is emitted at 0°. The η momentum is in general small and the condition of recoilless production of η is in fact reached at 900 MeV/c. Therefore, it appears that the (π^-,n) or the (π^+,p) reaction on a nuclear target could be used to search for any bound or resonant η-nuclear states. For such states to exist, the η-nucleus interaction has to be sufficiently attractive and, furthermore, the lifetime of η in a nucleus cannot be too short. It is encouraging that the ηN scattering length[14,15] indicates an attractive ηN interaction.

A comparison of the $\pi^- + {}^3He \to \eta + t$ reaction with the $\pi^+ + t \to \eta + {}^3He$ reaction could provide interesting information on the isospin-mixing of η. If η is in a pure I = 0 state, the exit channels can only couple to I = 1/2 and the cross section of these two reactions should be identical (after the correction of Coulomb interaction in the entrance channels). However, if η acquires an I = 1 component through isospin mixing, the cross section of these two reactions could be different enough to be observed.

High energy pions can also be used to produce other heavy mesons. The integrated cross sections[23] of the binary reactions $\pi^-p \to \rho n$ and $\pi^-p \to \eta' n$ are shown in Fig. 12. It is clear that higher energy machines, such as the proposed kaon factories, are required to

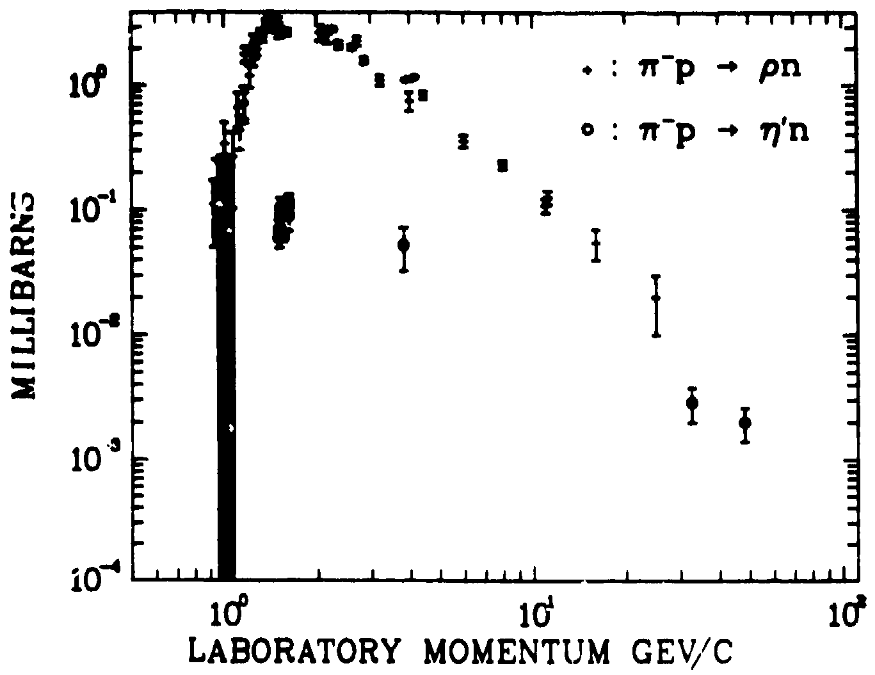

Fig. 12. Integrated cross section of the $\pi^- p \rightarrow \rho n$ and $\pi^- p \rightarrow \eta' n$ reactions.[23]

provide intense high energy pion beams. We believe that the study of short-lived heavy mesons is one of the many important subjects to be pursued at such accelerators.

ACKNOWLEDGEMENTS

I would like to thank my collaborators J. E. Simmons, J. Kapustinsky, N. Stein, D. H. Fitzgerald, and T. K. Li for their help and support in this experiment.

REFERENCES

1. Review of Particle Properties, Particle Data Group, 1984.
2. M. Gell-Mann, Caltech Report CTSL-20 (1961).
   S. Okubo, Prog. Theor. Phys. 27, 949 (1962).
3. A. Duane et al., Phys. Rev. Lett. 32, 425 (1974).
4. R. H. Dalitz and F. Von Hippel, Phys. Lett. 10, 153 (1964).
5. D. J. Gross, S. B. Treiman, and F. Wilczek, Phys. Rev. D19, 2188 (1979).
6. G. Segre and J. Weyers, Phys. Lett. 62B, 91 (1976).
7. R. E. Cutkosky, Phys. Lett. 88B, 339 (1979).
8. H. Harari, Phys. Lett. 60B, 172 (1976).
9. M. Gormley et al., Phys. Rev. Lett. 21, 402 (1968).
10. J. J. Thaler et al., Phys. Rev. Lett. 29, 313 (1972).
    M. R. Jane et al., Phys. Lett. 48B, 260 (1974).
11. F. Binon et al., Nuovo Cimento 71A, 497 (1982).

12. J. J. Thaler et al., Phys. Rev. D7, 2569 (1973).
13. J. D. Davies et al., Nuovo Cimento 24A, 324 (1974).
14. S. F. Tuan, Phys. Rev. 139, B1393 (1965).
15. R. S. Bhalerao and L. C. Liu, LANL Preprint, LA-UR-84-3384, to be published in Phys. Rev. Lett.
16. O. Dumbrajs et al., Nucl. Phys. B216, 277 (1983).
17. Landolt-Börnstein I/6, Elementary Particle Properties and Production Spectra (1972), Sects. 1.3.4; 1.5.5.
18. R. C. Chase et al., Phys. Lett. 30B, 659 (1969).
J. P. Boright et al., Phys. Lett. 33B, 615 (1970).
19. H. Becker et al., Nucl. Phys. B167, 292 (1980).
20. S. Ogawa et al., Suppl. Prog. Theor. Phys. 39, 140 (1967).
21. M. M. Nagels, T. A. Rijken, and J. J. de Swart, Phys. Rev. D15, 2547 (1977).
C. B. Dover and A. Gal, Prog. in Part. and Nucl. Phys. 12, 171 (1984).
22. W. W. Buck, C. B. Dover, and J. M. Richard, Ann. Phys. 121, 47 (1979).
23. V. Flaminio et al., CERN HERA 79-01 (1979).
24. F. Bulos et al., Phys. Rev. 187, 1827 (1969).
25. R. M. Brown et al., Nucl. Phys. B153, 89 (1979).
26. O. Guisan et al., Nucl. Phys. B32, 681 (1971).
27. V. V. Barmin et al., Sov. J. Nucl. Phys. 28, 780 (1979).
V. N. Bolotov et al., Sov. J. Nucl. Phys. 20, 504 (1975).
V. V. Arkhipov et al., Sov. J. Nucl. Phys. 39, 76 (1984).
V. D. Apokin et al., Sov. J. Nucl. Phys. 35, 219 (1982).
28. L. O. Abrahamian et al., Phys. Lett. 44B, 301 (1973).
29. H. Brody et al., Phys. Rev. D9, 1917 (1974).
30. R. Frascaria et al., Proceeding 9th ICOHEPANS, VERSAILLES (1981).
31. LAMPF proposal E852, "Measurement of $(\pi^{\pm},\eta)$ Reactions on Nuclear Targets to Study the Production and Interaction of η-Mesons with Nuclei," Spokesman: J. C. Peng.
32. LAMPF proposal E934, "Inclusive (π,η) Reactions in Nuclei," Spokesmen: J. C. Peng and J. E. Simmons.
33. "Pion Production and Absorption in Nuclei: 1981," AIP Conf. Proc. No. 79 (1982).
34. A. Shor et al., Phys. Rev. Lett. 48, 1597 (1982).
35. P. Braun-Munzinger et al., Phys. Rev. Lett. 52, 255 (1984).
36. LAMPF Users' Handbook.
37. H. W. Baer et al., Nucl. Instr. Meth. 180, 445 (1981).
38. E. P. Colton et al., Nucl. Instr. Meth. 178, 95 (1980).
39. L. C. Liu and R. S. Bhalerao, unpublished (1985).
40. D. J. Herndon et al., πN Partial-Wave Amplitudes, LBL Report UCRL-20030.
R. A. Arndt, Phase Shift Solution FP84.
41. D. H. Fitzgerald, private communication.
42. J. C. Peng et al., "A Proposed Experimental Program to Study η-Production, η-Decay and η-Nucleus Interactions at LAMPF," LANL Report, LA-9923-MS (1983).